Analytical Solution for Duct Mode Propagation inUniform Flow

Swirl Validation

Jeff Severino

This document shows the analytical duct mode solution as well as a numerical comparison.

Mechanical, Industrial, Manufacturing Engineering Department
University Of Toledo
Toledo, OH
October 20, 2022

0.1 Introduction - Turbomachinery Noise

Turbomachinery noise generation occurs from pressure fluctuations from the series of fans within it's annular duct. While the jet that is produced from this stream of air freely radiates to the observer, the pressure fluctuations produced from the rotor may or may not propagate out of the inlet and exhaust and radiate to the observer. The production of this propagation can be characterized by standing waves referred to as modes, in particular, duct modes because the mode itself is dependent on the geometry of the column of air within the annular duct, as well as the speed of the flow moving through it

0.2 Duct Modes

The pressure field within a duct is governed by the convective wave equation, a second order ODE as a function of radius. Goldstein's *Aeroacoustics* shows that the wave equation can be obtained by taking the divergence of the momentum equation and subtracting the material derivative of the continuity equation, however, the same equation can be obtained by resubstitution of the continuity and momentum equations into the energy equations after the fluctuations have also been substituted for the primative variables. (See Appendix for derivation)

The solution of the convective wave equation are eigenvalues and eigenvectors which may or may not correspond to acoustic disturbances fall into two groups. One group corresponding to the acoustics propagation and the other group corresponding to the convection speed of the flow. Both are modes that are a result from the pressure distribution from within the cylindrical domain.

Modes can be categorized based on the sign of the axial wavenumber and if it is complex in value. For example, for the uniform axial flow case, propagating modes are defined by axial wavenumbers, k_x, that have a real-part only, yielding the assumed fluctuation to resemble Euler's Formula ($e^{ik_x x}$). On the other hand, if the k_x is complex, then the mode will resemble an exponentially decaying function since the imaginary number cancels, leaving a minus sign in front of the axial wavenumber. These two distinctions are referred to as "cut-on" and "cut-off" in the field of ducted sound propagation. Furthermore, the sign of the imaginary part will change the direction of the mode's decay. If k_x is positive, the decay rate occurs in the negative direction. Conversely, if k_x is negative, the decay occurs in the positive direction. The axial wavenumber for uniform axial flow is,

$$k_x = \frac{-M_x k \pm \sqrt{k^2 - (1 - M_x^2) J'^2_{m,n}}}{(1 - M_x^2)}. \tag{1}$$

where M_x is the axial Mach number, k is the temporal (referred to as reduced) frequency, and $J'_{m,n}$ is the derivative of the Bessel function of the first kind. The $\pm$ accounts for both upstream and downstream modes.

The condition for propagation is such that the axial wavenumber is larger than a "cut-off" value

$$k_{x,real} = \frac{\pm M_x k}{(M_x^2 - 1)}. \tag{2}$$

Every term that is being raised to the one half i.e. square rooted must be larger than zero to keep axial wavenumber from being imaginary. The mode will propagate or decay based on this condition. Recall thaT the mode is of the form

$$e^{ik_x x} \tag{3}$$

if k_x has a real part, $k_{x,real}$ and an imaginary part $ik_{x,imag}$ then,

$$= e^{ik_x x} \tag{4}$$

$$= e^{i(k_{x,real}+ik_{x,imag})x} \tag{5}$$

$$= \underbrace{e^{ik_{x,real}x}}_{amplitude} \quad \underbrace{e^{-k_{x,imag}x}}_{exponential\ decay} \tag{6}$$

Although the "cut-off" decay to nearly zero rapidly, the rate at which this occured was not much of a concern earlier on in turbomachinery design. As nacelles continue to grow shorter, a mode that is "cut-off" may make it outside the duct.

For this work a desired amplitude was arbitrarily chosen for a mode, $y_{desired}$ and then the axial location at which this occurred, $x_{desired}$ which can be compared against a desired length for a nacelle. Since SWIRL assumes an infinitely long duct, there is nothing limiting the modes propagation with respect to nacelle length. For example, if the desired amplitude is one percent, then $x_{desired}$ is 0.46,

$$\begin{aligned} 0.01 &= e^{-10x_{desired}}, \\ -\frac{ln|0.01|}{10} &= x_{desired}, \\ -\frac{ln|0.01|}{10} &= 0.4605170185988091. \end{aligned}$$

0.3 Analytical Test Case

σ	*0.0*
k	*10*
m	*2*
M_x	*0.3*

Table 1: Validation test case parameters, Uniform Flow Annular Duct

0.3.1 Axial Wavenumber

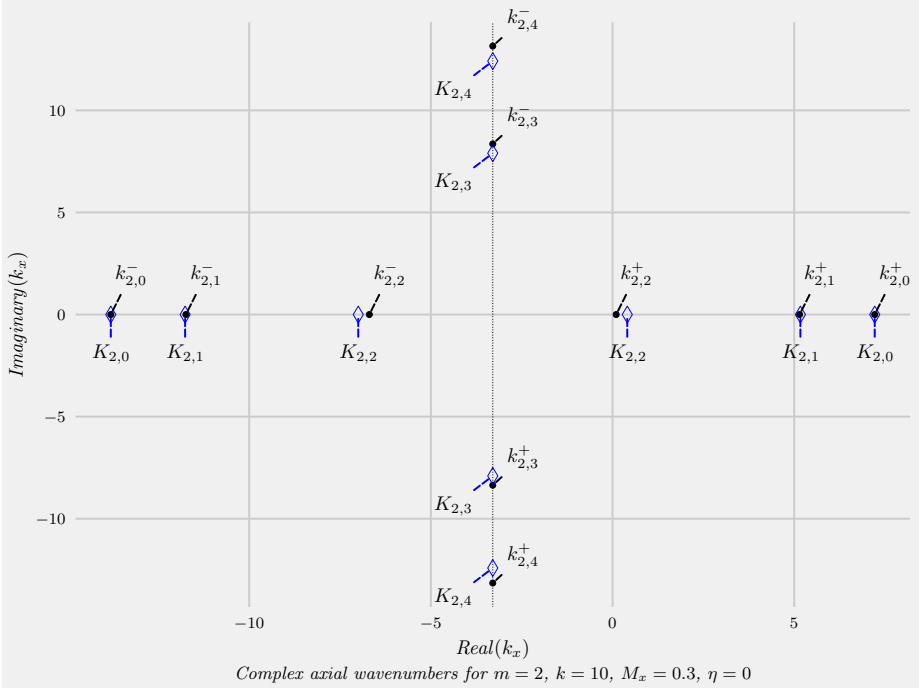

Figure 1: Second Order, Analytical Solution vs Numerical Approximation using 33 points

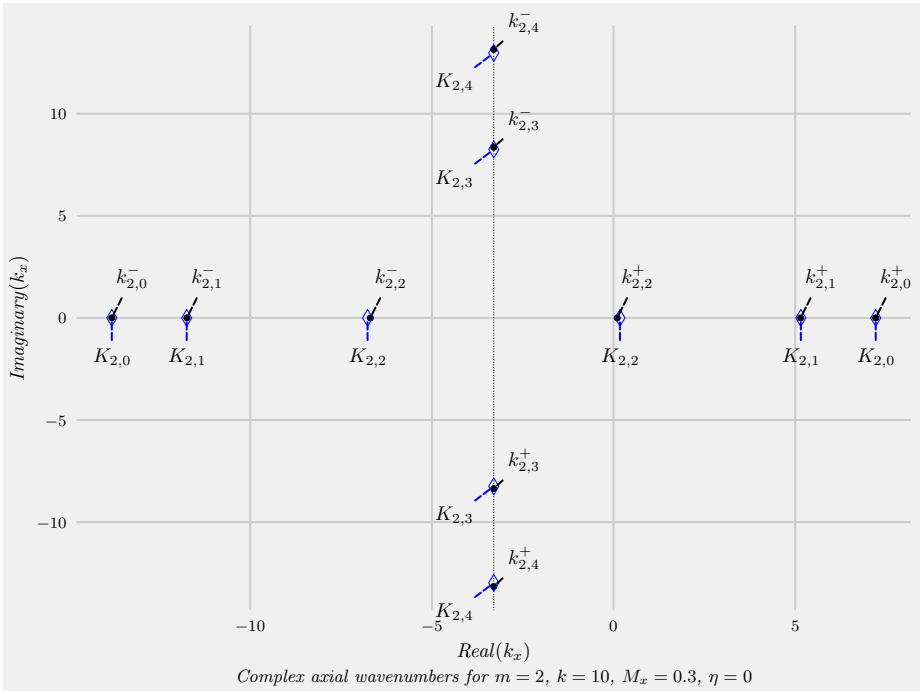

Figure 2: Second Order, Analytical Solution vs Numerical Approximation using 66 points

0.3.2 Propagating Radial Modes

Second Order, Radial Mode 0

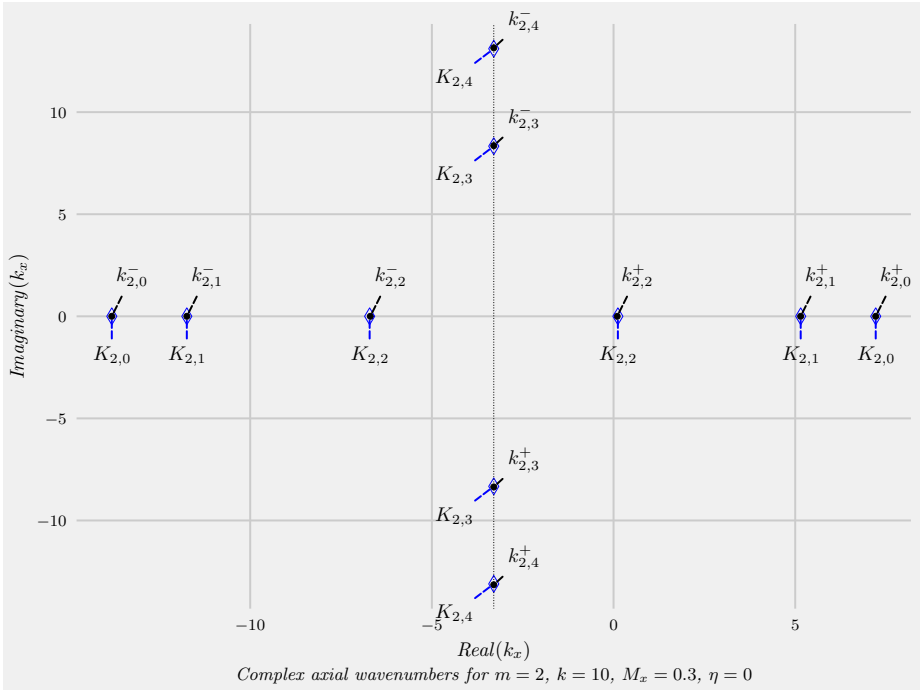

Figure 3: Second Order, Analytical Solution vs Numerical Approximation using 132 points

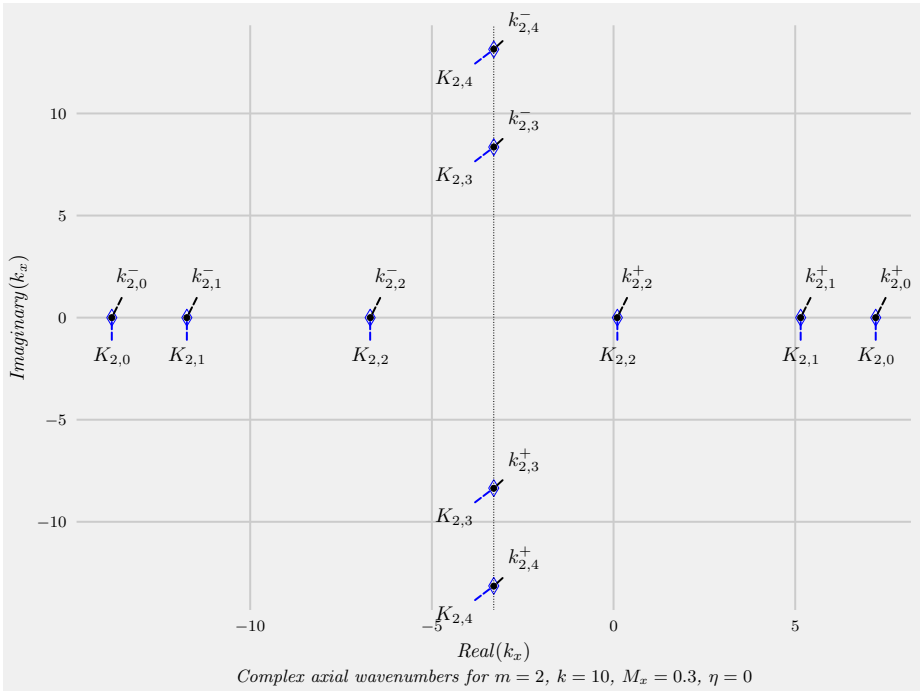

Figure 4: Second Order, Analytical Solution vs Numerical Approximation using 264 points

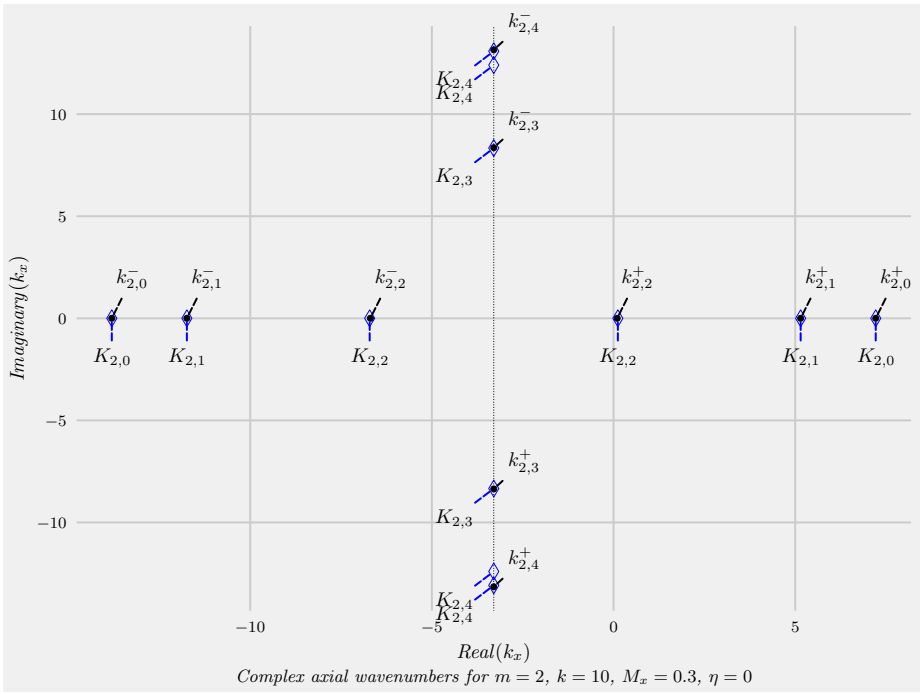

Figure 5: Fourth Order, Analytical Solution vs Numerical Approximation using 33 points

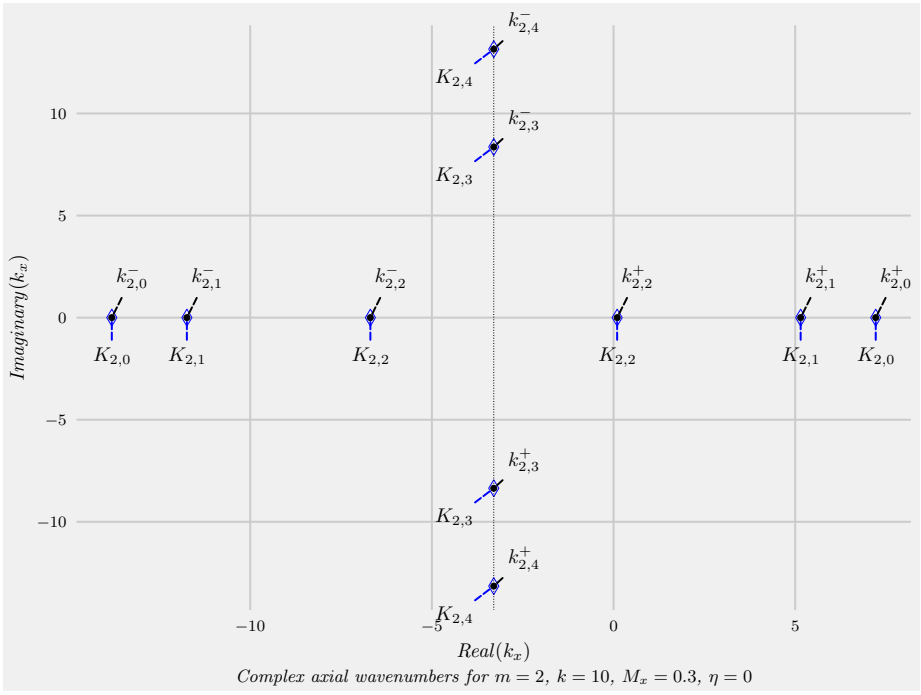

Figure 6: Fourth Order, Analytical Solution vs Numerical Approximation using 66 points

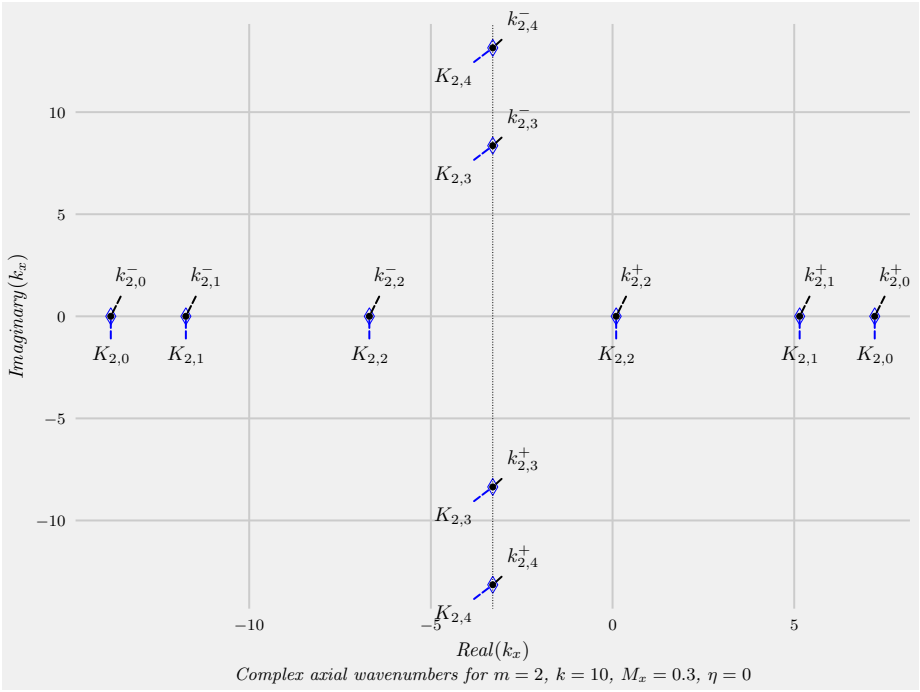

Figure 7: Fourth Order, Analytical Solution vs Numerical Approximation using 132 points

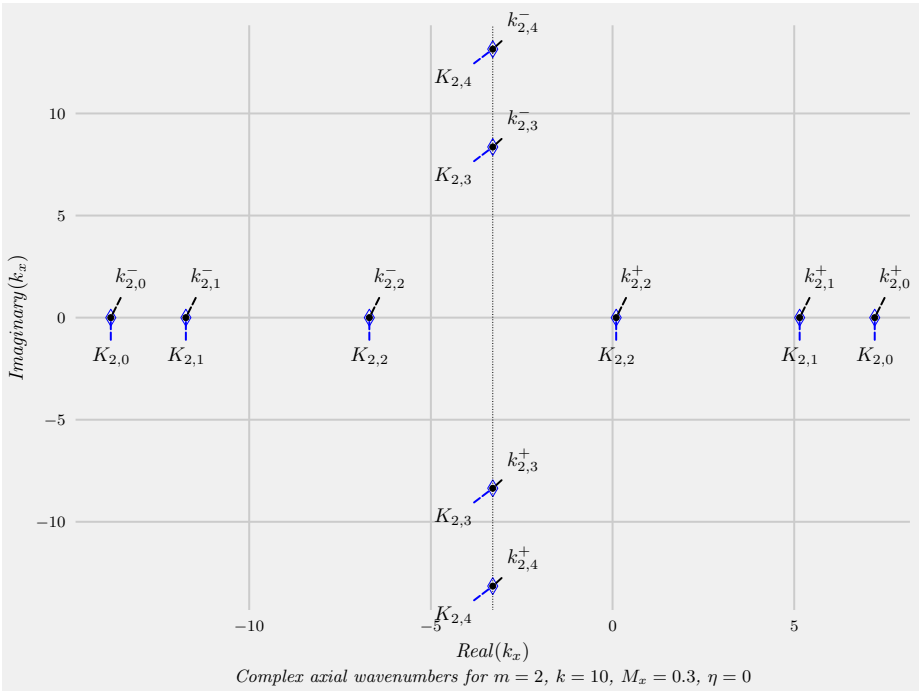

Figure 8: Fourth Order, Analytical Solution vs Numerical Approximation using 264 points

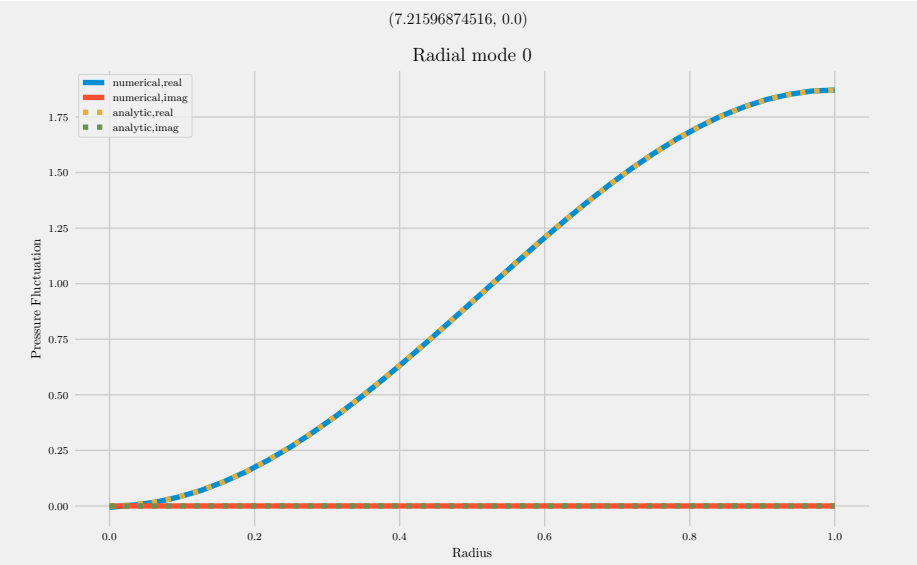

Figure 9: Second Order, Case number 0, 33points

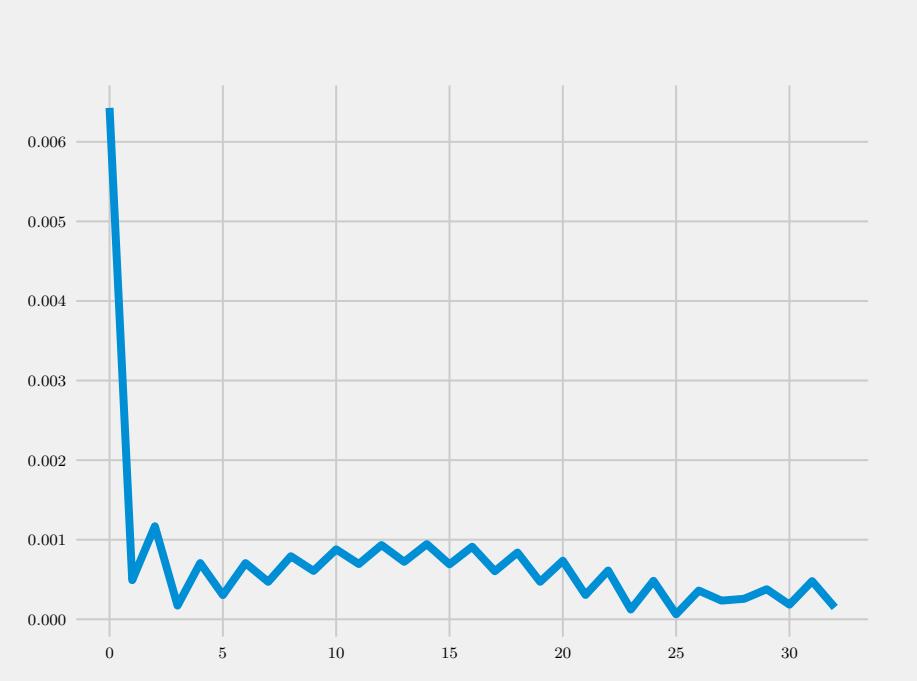

Figure 10: Second Order, Case number 0, 33points

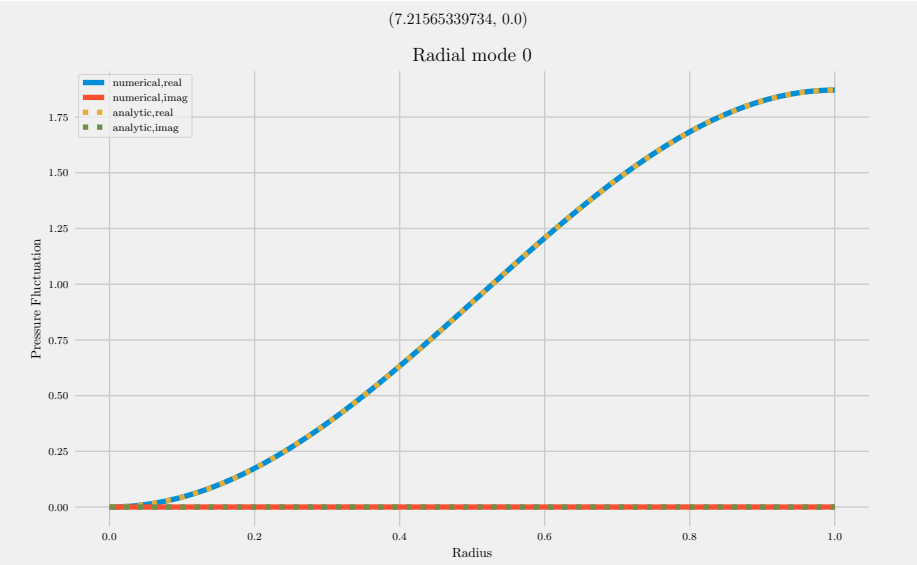

Figure 11: Second Order, Case number 0, 66points

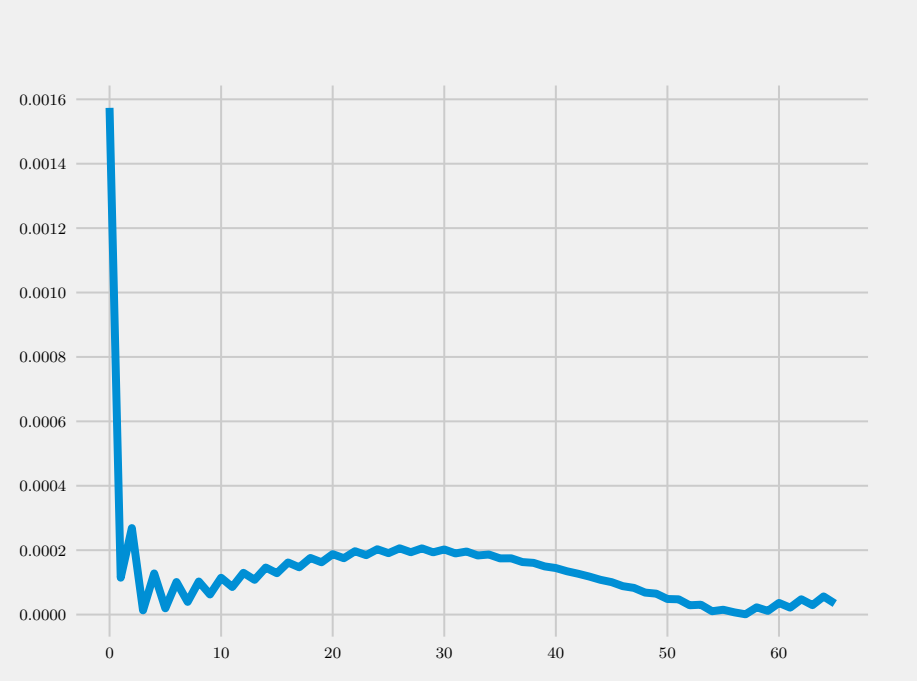

Figure 12: Second Order, Case number 0, 66points

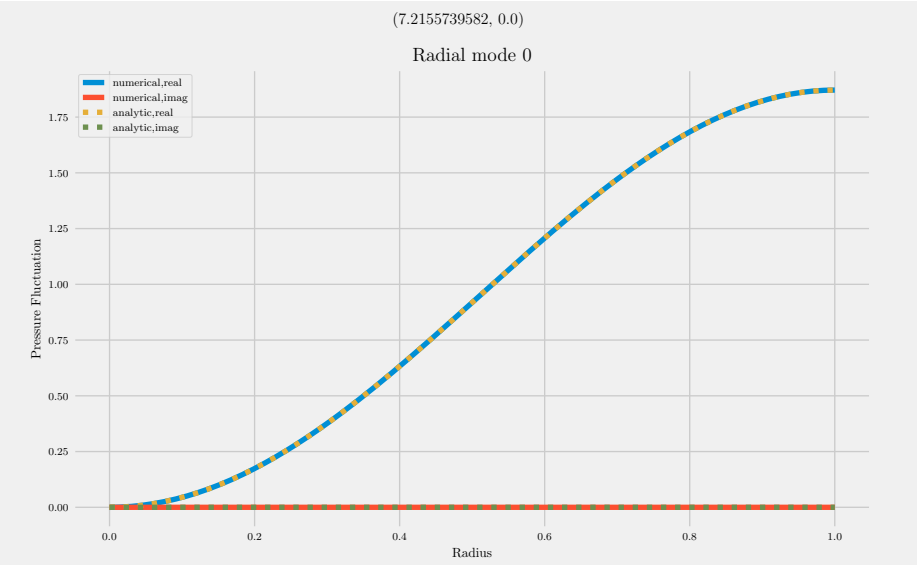

Figure 13: Second Order, Case number 0, 132points

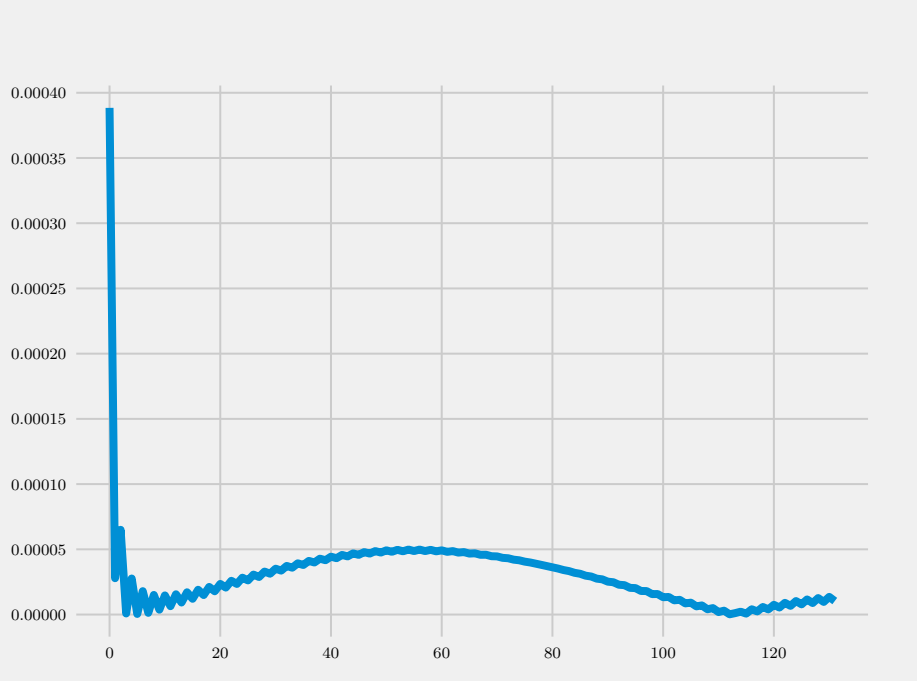

Figure 14: Second Order, Case number 0, 132points

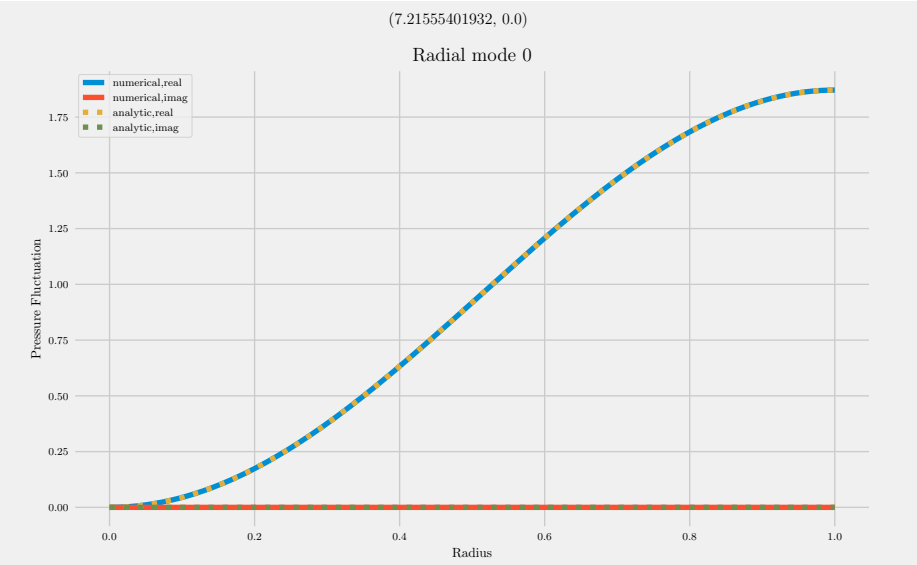

Figure 15: Second Order, Case number 0, 264points

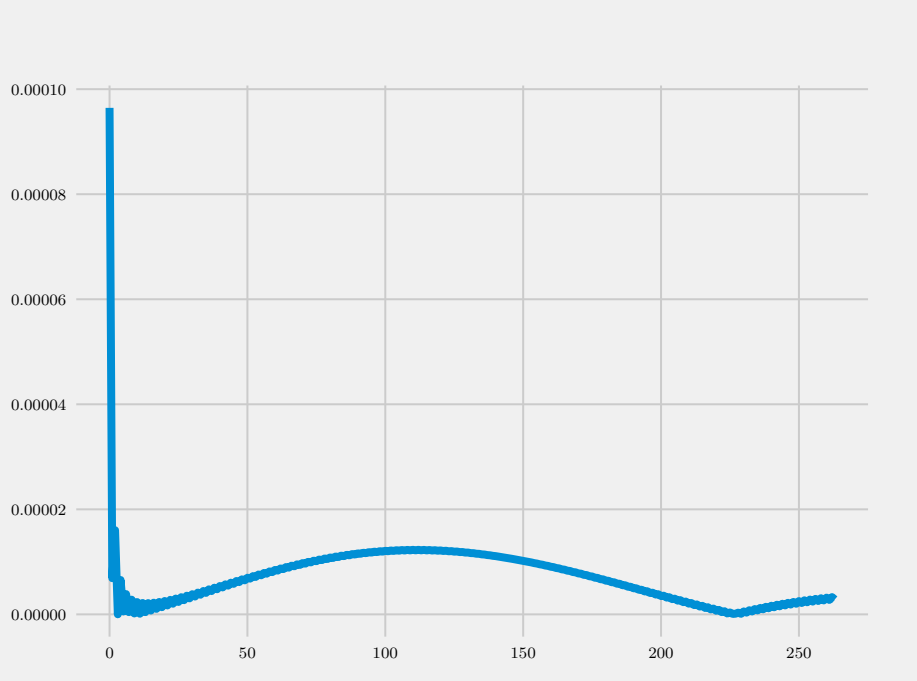

Figure 16: Second Order, Case number 0, 264points

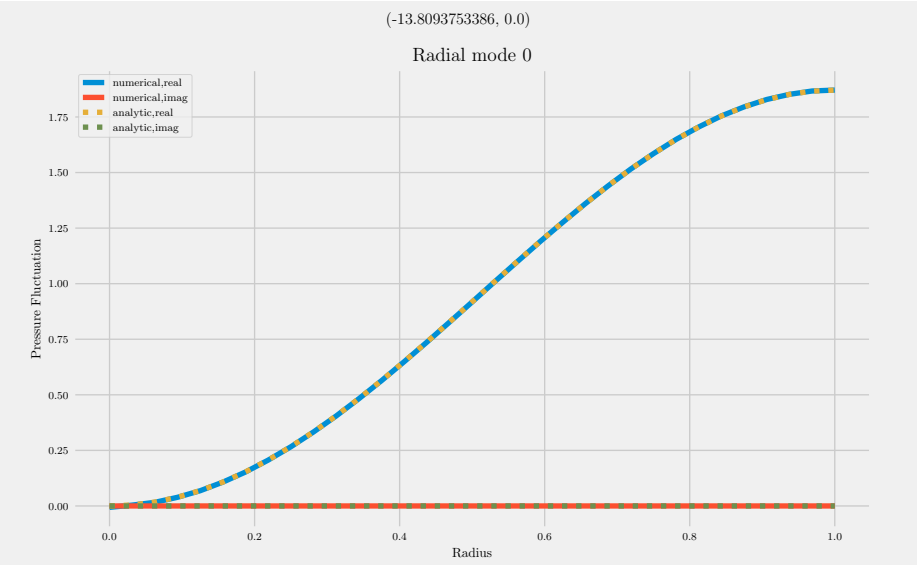

Figure 17: Second Order, Case number 1, 33points

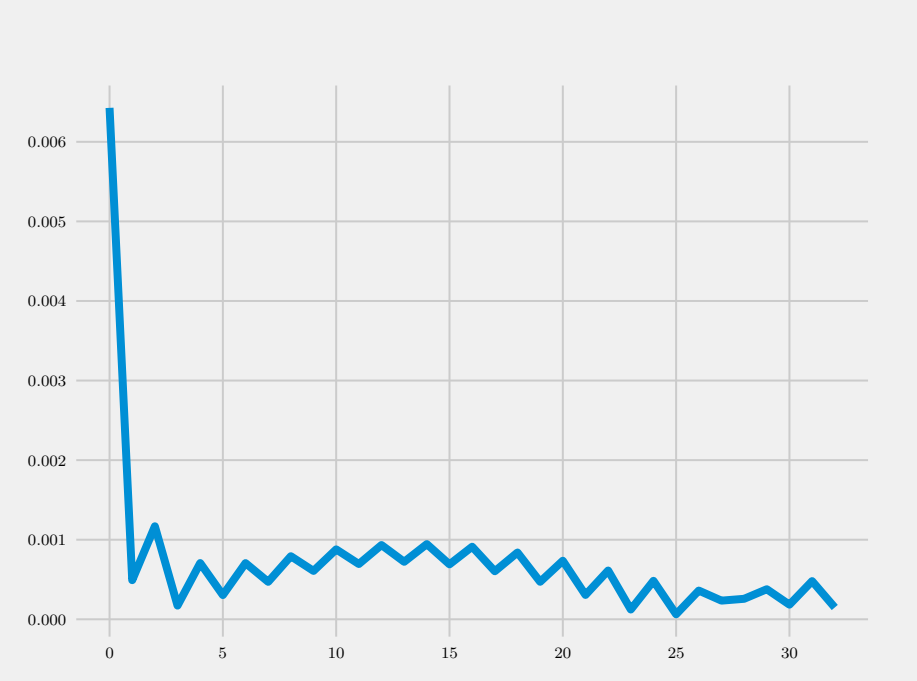

Figure 18: Second Order, Case number 1, 33points

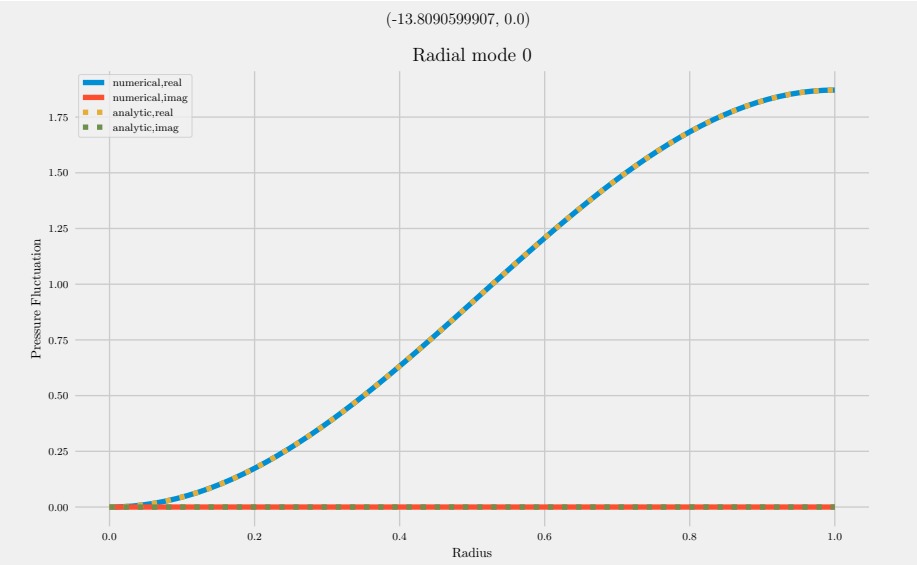

Figure 19: Second Order, Case number 1, 66points

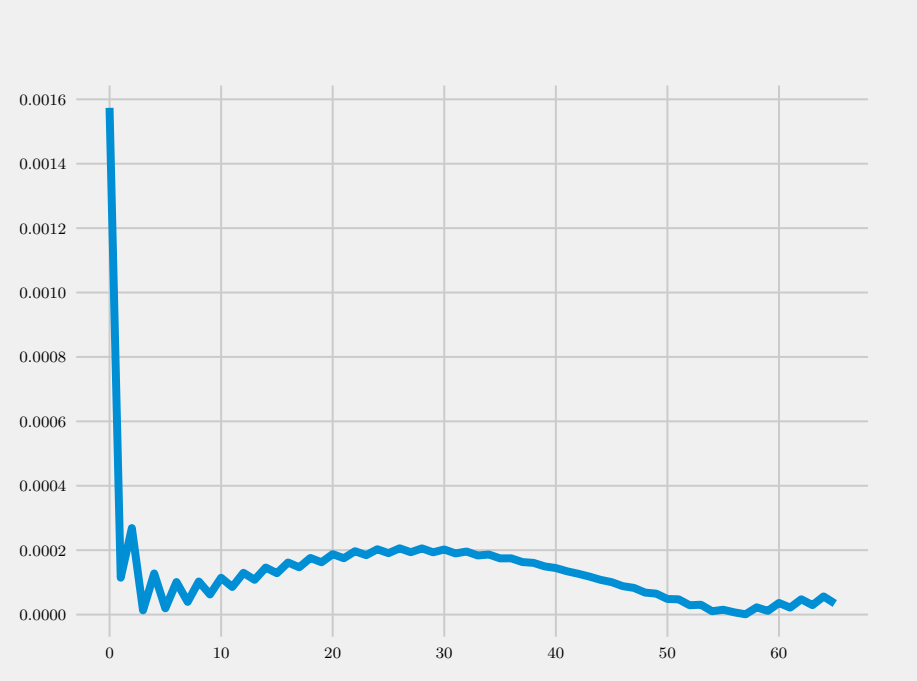

Figure 20: Second Order, Case number 1, 66points

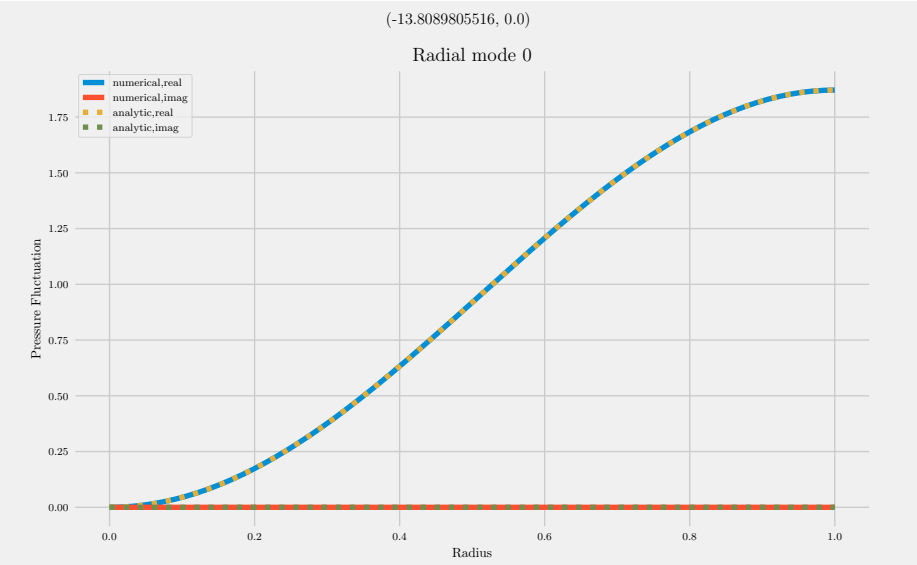

Figure 21: Second Order, Case number 1, 132points

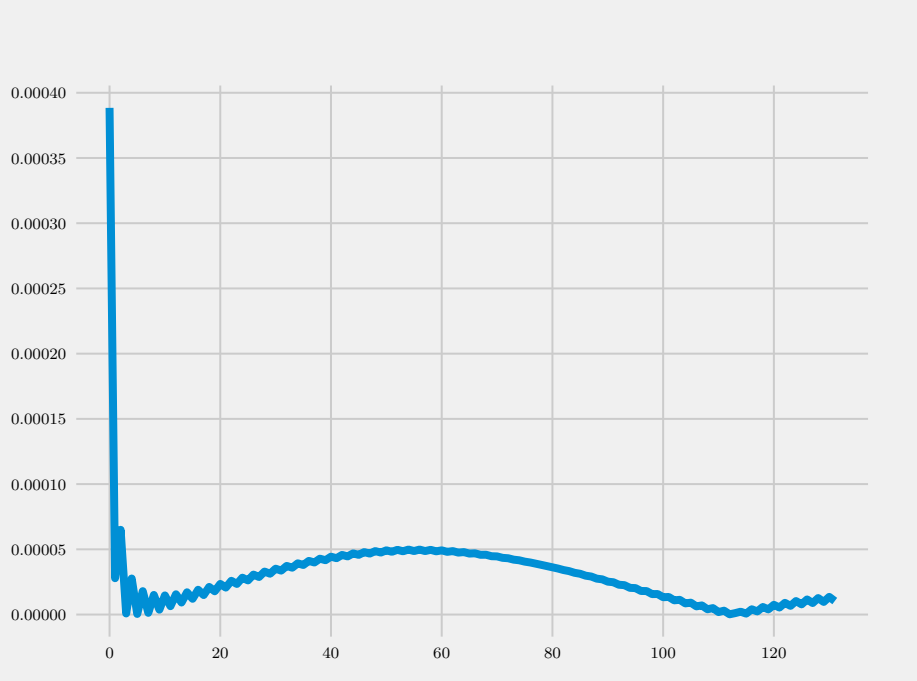

Figure 22: Second Order, Case number 1, 132points

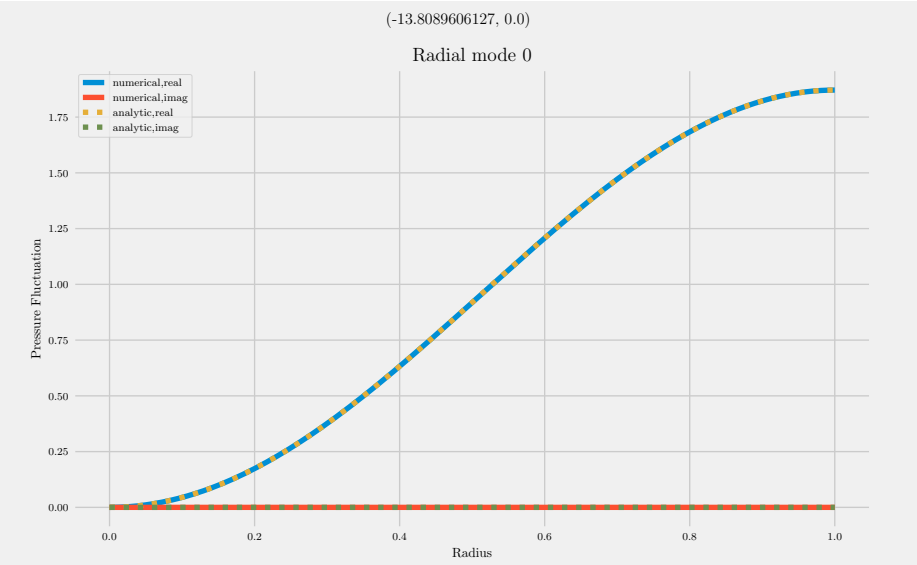

Figure 23: Second Order, Case number 1, 264points

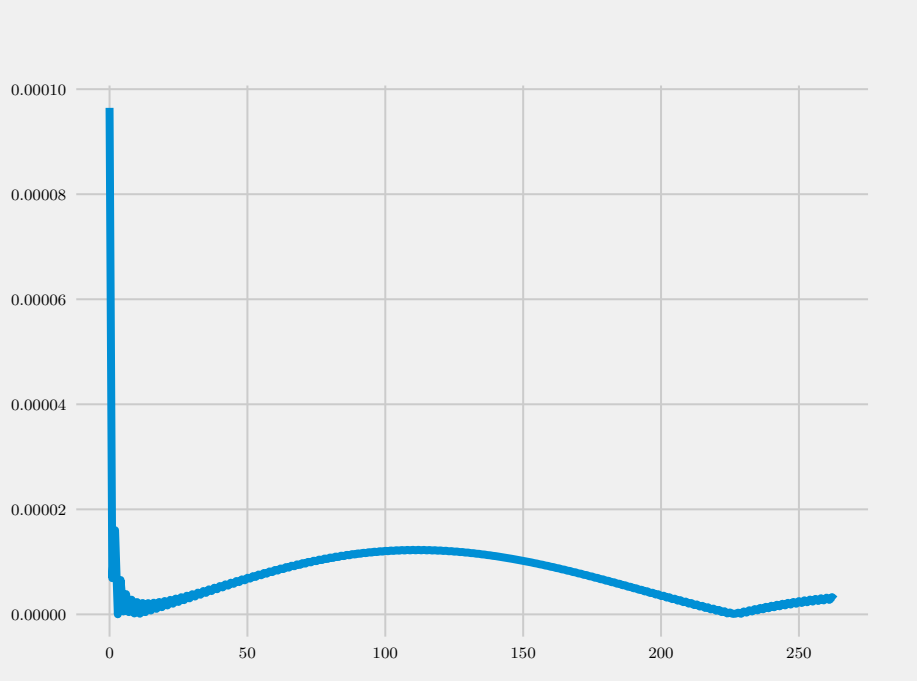

Figure 24: Second Order, Case number 1, 264points